McCarl et al. Supplemental Figure 1

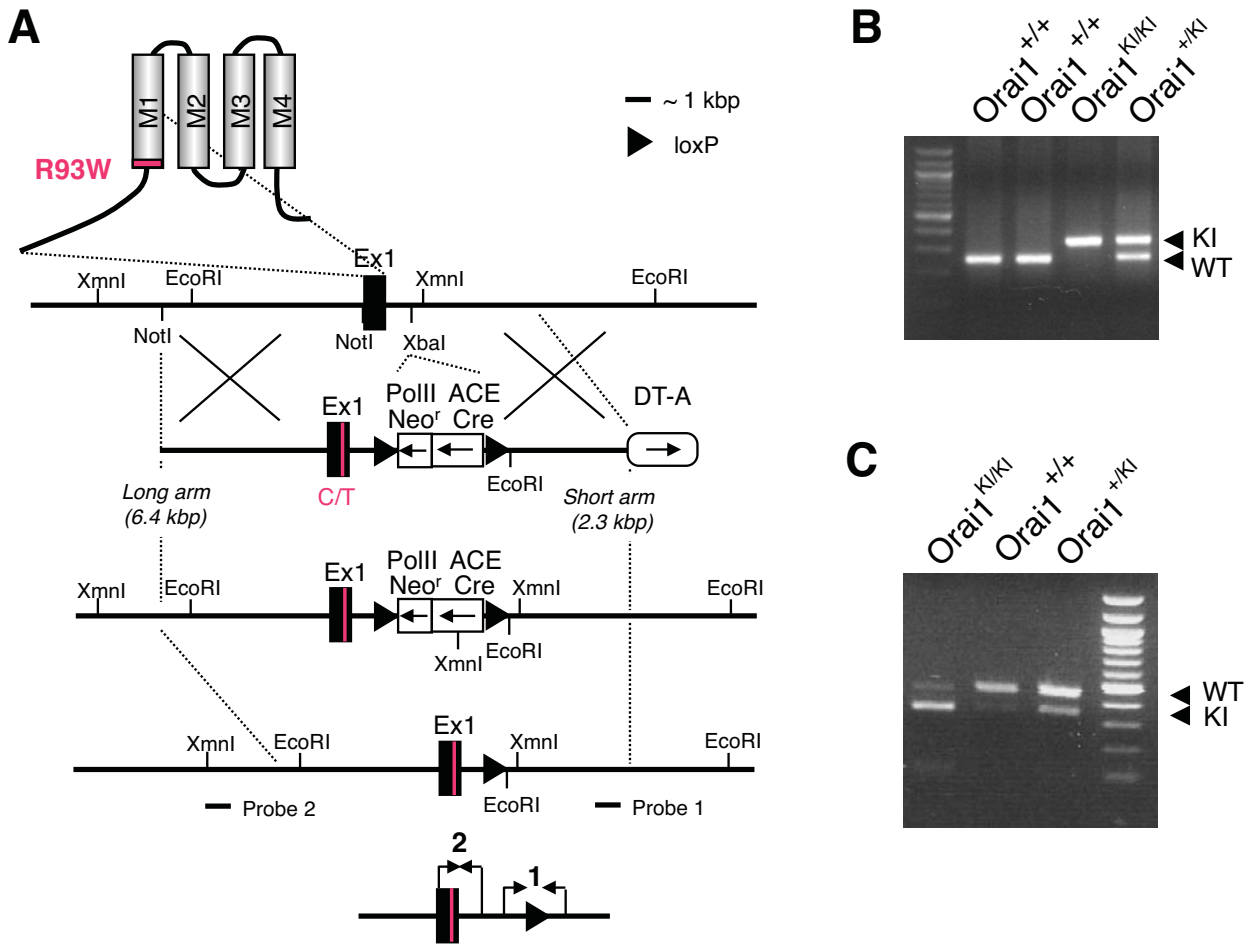

Generation of *Orai1*^{R93W} knock-in mice (*Orai1*$^{KI/KI}$).
A, Gene targeting of the *Orai1 g*ene by homologous recombination. For details see Materials and Methods. Briefly, codon 93 (CGG encoding R93) in exon 1 of the *Orai1* gene was replaced with TGG (encoding W93). A Neo cassette in the targeting vector used for selection of ES cells was deleted by Cre expression under the control of the testis specific ACE promoter during spermatogenesis in chimeric mice. ACE, angiotensin-converting enzyme; DT-A, diptheria toxin A; PolII, DNA polymerase II. This panel was originally published in: Bergmeier et al. "R93W mutation in Orai1 causes impaired calcium influx in platelets". *Blood*. 2009;113: 675-678. © the American Society of Hematology. **B**, Successful gene-targeting was confirmed by PCR using a primer pair (indicated as "1" in panel A) flanking the remaining loxP site in the *Orai1* locus as indicated in A. The "floxed" locus generates a 320 bp band compared to a 280 bp band for the wild-type locus. **C**, Successful gene-targeting in *Orai1*$^{KI/KI}$ mice was confirmed, in addition, by restriction digests of PCR products from *Orai1*$^{KI/KI}$ and wild-type *Orai1*$^{+/+}$ mice using a second primer pair (indicated by "2" in panel A). The mutated codon 93 (TGG) creates a recognition site for the restriction endonuclease PvuII (CAGCTG). PvuII digest of PCR products (453 bp) generates two bands (346 and 107 bp) in *Orai1*$^{KI/KI}$ mice compared to a single undigested band (453 bp) in wild-type mice.

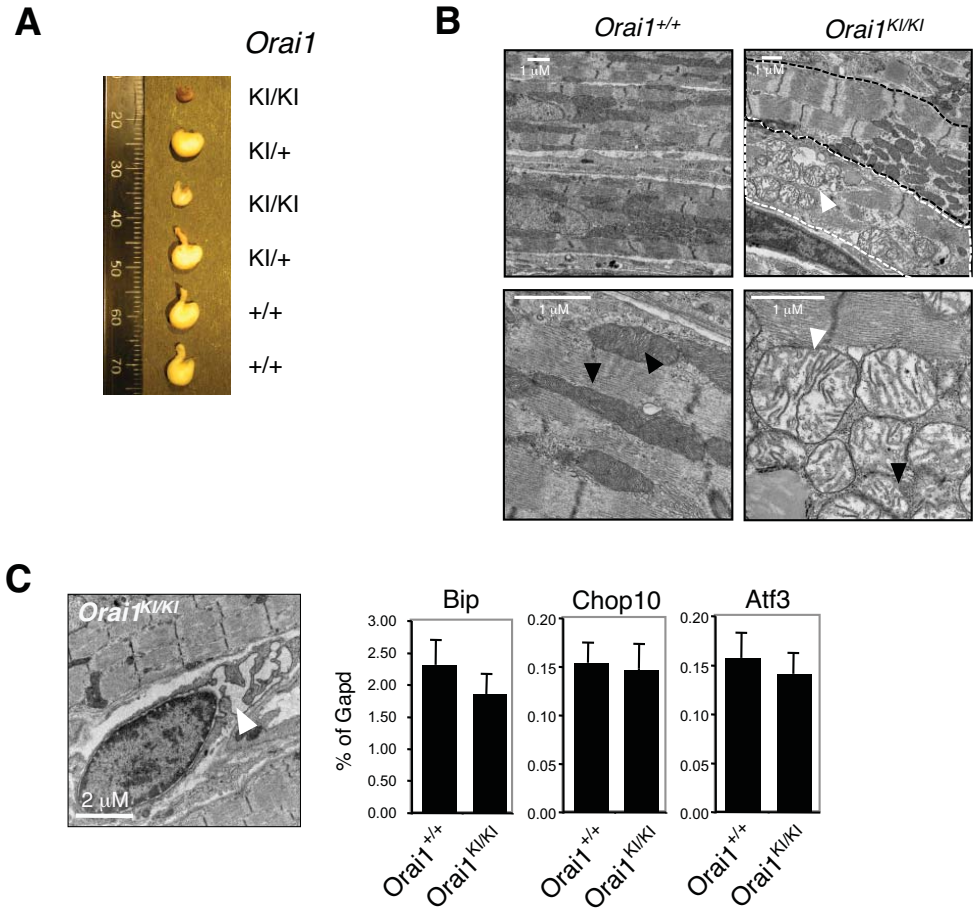

Impaired feeding, lack of ER stress and localized mitochondriopathy in cardiomyocytes of *Orai1*$^{KI/KI}$ mice.

A, Inability to feed and dehydration in *Orai1*$^{KI/KI}$ pups. 6-12h after birth, *Orai1*$^{KI/KI}$ (ICR N4f2) pups showed no or small milk patches upon visual inspection of live mice or following dissection compared to *Orai1*$^{KI/+}$ or *Orai1*$^{+/+}$ littermates. *Orai1*$^{KI/KI}$ pups died within 12h post partum and appeared severely dehydrated. **B**, Ultrastructural abnormalities in cardiomyocytes of *Orai1*$^{KI/KI}$ mice. Hearts from surviving *Orai1*$^{KI/KI}$ (ICR N3f2) and littermate *Orai1*$^{+/+}$ mice were analyzed for cellular abnormalities on day 5 post partum by transmission electron microscopy. Note the large number of dilated mitochondria with dissolved cristae structure in a fraction of cardiac muscle fibers from *Orai1*$^{KI/KI}$ but not *Orai1*$^{+/+}$ control mice. Magnification 4,400x (top panels), 25,000x (bottom panels). **C**, *Left,* A minority (< 5%) of fibroblasts in skeletal muscle from *Orai1*$^{KI/KI}$ mice show dilated ER and nuclear envelopes (magnification 5,600x). *Right,* Genes linked to ER stress are not upregulated in *Orai1*$^{KI/KI}$ mice. RNA was isolated from skeletal muscles of the lower extremity of *Orai1*$^{KI/KI}$ (ICR N3f2) and littermate *Orai1*$^{+/+}$ mice 5 days post partum and expression levels of genes associated with ER stress were analyzed by quantitative real-time PCR. Expression levels of ER stress associated genes Bip, Chop10 and Atf3 were normal compared to littermate controls. Averages (±SEM) of 8 repeat experiments are shown.

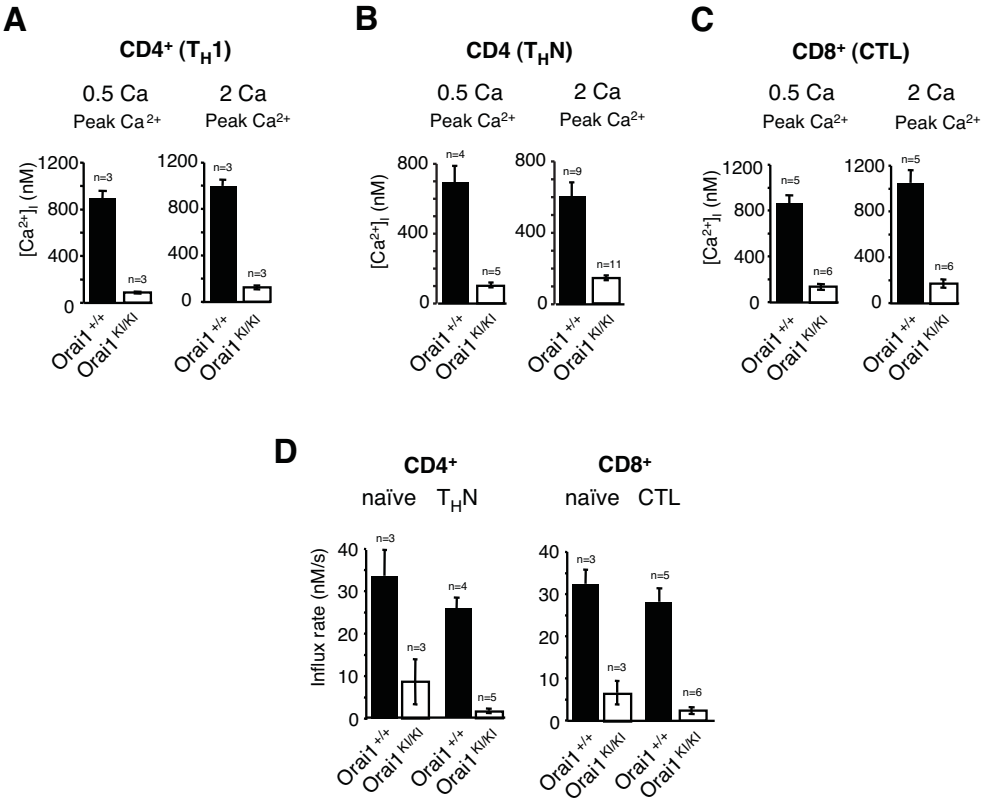

Quantification of store-operated Ca^{2+} entry in T and B cells from *Orai1*$^{KI/KI}$ mice.
Peak $[Ca^{2+}]_i$ and initial rates of Ca^{2+} influx in naïve and differentiated T cells are averages of experiments shown in Fig. 2-3. **A-C**, Peak $[Ca^{2+}]_i$ in *in vitro* differentiated T_H1 cells, T_HN cells and cytotoxic T lymphocytes (CTL) was determined after readdition of 0.5 mM and 2 mM Ca^{2+} Ringer solution following stimulation with 1 μM thapsigargin. **D**, Comparison of initial rates of Ca^{2+} influx in TG stimulated naïve vs. differentiated $CD4^+$ and $CD8^+$ T cells following readdition of 0.5 mM Ca^{2+}_o. Note that SOCE is more severely impaired in differentiated compared to naïve T cells. For experimental details see Fig. 2-3. 80-100 cells per experiment were analyzed. Error bars, SEM.

McCarl et al. Supplemental Figure 4

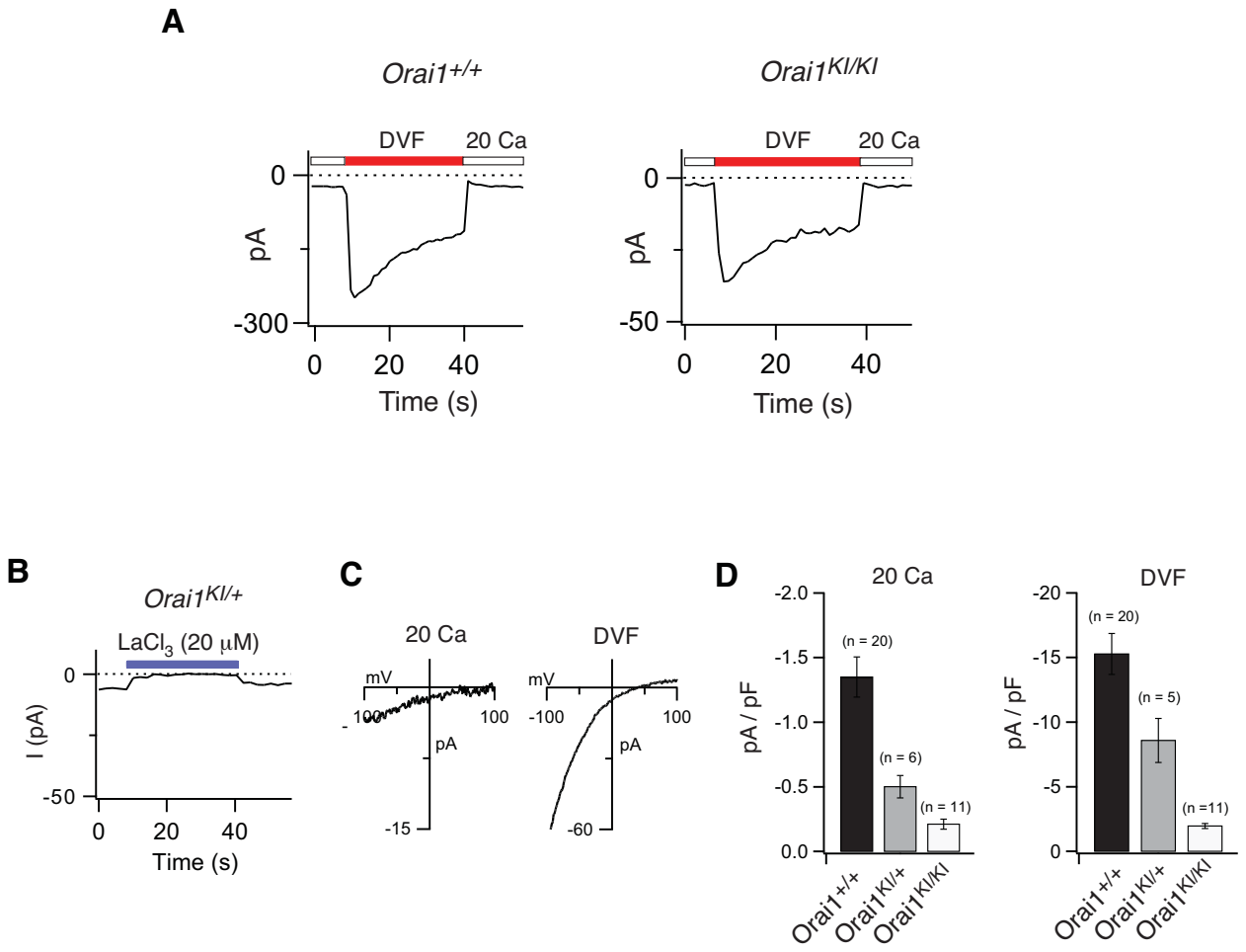

Properties of CRAC currents in T cells from *Orai1*$^{KI/KI}$, *Orai1*$^{KI/+}$ and *Orai1*$^{+/+}$ mice.
Ca^{2+} and Na^{+} currents were recorded in *in vitro* differentiated $CD4^{+}$ T_HN cells from *Orai1*$^{+/+}$ control, *Orai1*$^{KI/KI}$ and *Orai1*$^{KI/+}$ mice. T cells were stimulated with thapsigargin to activate CRAC channels. **A**, Leak-corrected currents measured during hyperpolarizing pulses to -100 mV are plotted against time. The extracellular solution was switched between 20 mM Ca^{2+} (open bar) and Na^{+}-based divalent free solution (DVF, red bars). Note that residual currents in T cells from *Orai1*$^{KI/KI}$ mice show similar behaviour as those in wildtype T cells with regard to the increase in current amplitude upon switching from Ca^{2+} Ringer solution to DVF solution and depotentiation of the monovalent currents in DVF over tens of seconds. **B-C**, Residual Ca^{2+}-I_{CRAC} in $CD4^{+}$ T cells from heterozygous *Orai1*$^{KI/+}$ mice is blocked by La^{3+} (B) and has inwardly rectifying current properties (C). Currents were recorded in 20 mM Ca^{2+}_o and DVF, respectively. 20 μM La^{3+} was added as indicated in the figure. **D**, Summary of current amplitudes recorded in T cells from *Orai1*$^{+/+}$ control, *Orai1*$^{KI/KI}$ and *Orai1*$^{KI/+}$ mice in 20 mM Ca^{2+}_o and DVF, respectively. Error bars, SEM.

McCarl et al. Supplemental Figure 5

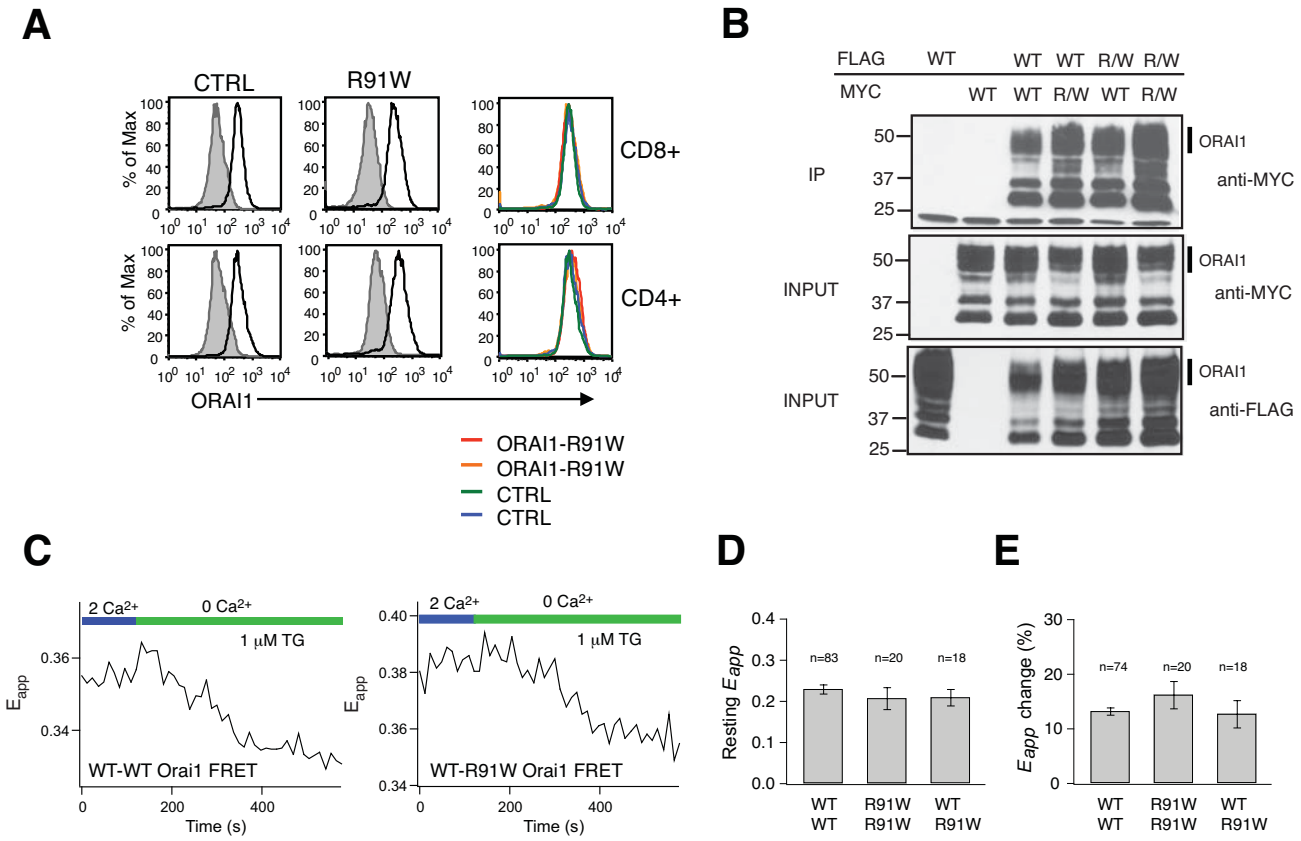

Mutant ORAI1-R91W protein is expressed and interacts with wild-type ORAI1.
A, Normal expression levels of ORAI1-R91W protein in T cells. For flow cytometry, $CD4^+$ and $CD8^+$ T cells from patients with ORAI1-R91W mutation and two healthy controls (CTRL) were stained with antibodies against CD4, CD8 and ORAI1 (black traces in left and middle panels) or PE-Cy5.5-labeled secondary antibody alone (gray shaded traces). Equal expression of wild-type and mutant ORAI1-R91W in $CD4^+$ and $CD8^+$ T cells is shown in overlay graphs (right panels). One representative experiment of 2 is shown. **B**, ORAI1-R91W can be immunoprecipitated with wild-type ORAI1. For coimmunoprecipitation experiments, MYC- and FLAG-tagged wildtype ORAI1 and mutant ORAI1-R91W were expressed in HEK293 cells. At 48 h after transfection, total cell lysates were prepared, incubated with anti-FLAG antibody, crosslinked to protein A beads and separated by SDS-PAGE. Coprecipitation of ORAI1 was detected with anti-MYC antibody. For the input control, cell lysates were separated by SDS-PAGE and incubated with anti-FLAG or anti-MYC antibody. One representative experiment of two is shown. **C**, ORAI1-R91W interacts with wild-type ORAI1 by FRET. HEK293 cells were transfected with wild-type ORAI1-CFP and either wild-type ORAI1-YFP or ORAI1-R91W-YFP together with mCherry–STIM1. ORAI1-ORAI1 FRET was measured in resting cells in 2 mM Ca^{2+}_o and following store depletion triggered by 1 μM TG applied in 0 mM Ca^{2+}_o. **D-E**, Summary of resting 3-cube E_{app} levels in 2 mM Ca^{2+}_o (D) and of the changes in E_{app} following store depletion with TG in 0 mM Ca^{2+}_o (E) in cells expressing wild-type ORAI1 alone (n = 83 cells), ORAI1-R91W alone (n = 20 cells) or wild-type ORAI1 and ORAI1-R91W together (n = 18 cells). Note that resting FRET levels and the decline in ORAI1-ORAI1 FRET following store depletion (described in Navarro-Borelly J Physiol 2008; 586:5383-5401) are comparable in cells expressing the various combinations of proteins indicating that the interaction of mutant ORAI1-R91W with wild-type ORAI1 is not impaired.

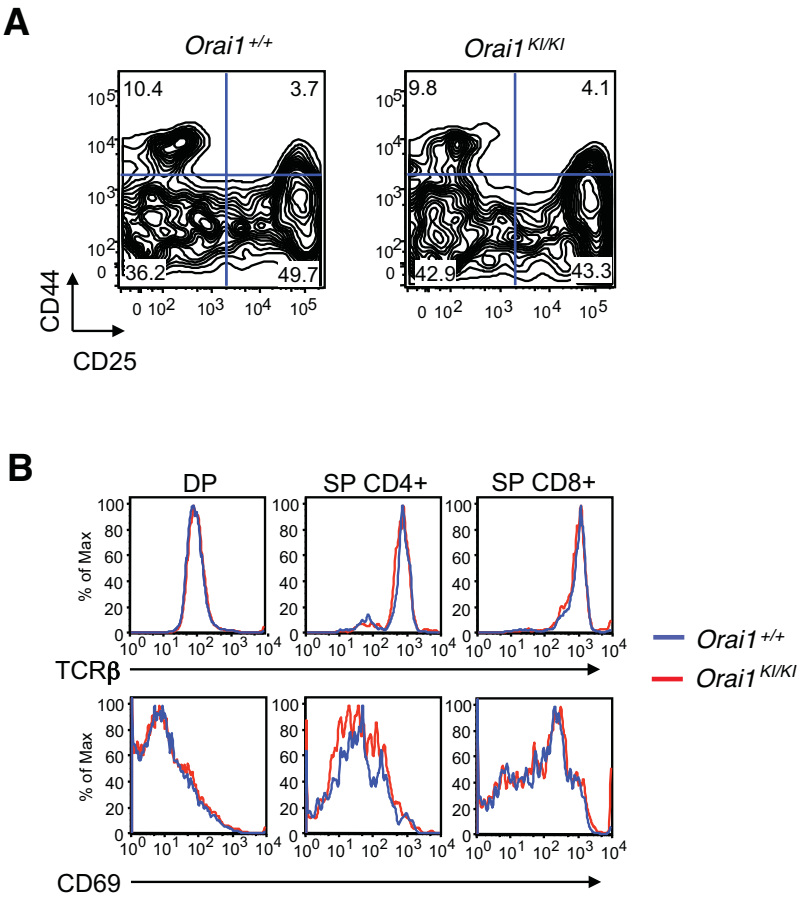

Normal T cell develoment in *Orai1*$^{KI/KI}$ mice.
Thymocytes were isolated from *Orai1*$^{KI/KI}$ and *Orai1*$^{+/+}$ fetal liver chimeric (FLC) mice 5-6 weeks after transfer of fetal liver cells to *Rag2*$^{-/-}$, $\gamma c^{-/-}$ mice. **A,** T cells were stained with antibodies to CD4, CD8, CD25 and CD44 and analyzed by flow cytometry. Shown is one representative experiment of three depicting thymocyte development in *Orai1*$^{KI/KI}$ and *Orai1*$^{+/+}$ control FLC mice at the CD4$^-$CD8$^-$ (DN) stage. Note the comparable distribution of immature T cells at the DN1 (CD44$^+$CD25$^-$), DN2 (CD44$^+$CD25$^+$), DN3 (CD44$^-$CD25$^+$), and DN4 (CD44$^-$CD25$^-$) stage in *Orai1*$^{KI/KI}$ and *Orai1*$^{+/+}$ control mice. **B**, Normal expression of TCRβ chain and CD69 on immature thymocytes. Thymocytes from *Orai1*$^{KI/KI}$ (red) and *Orai1*$^{+/+}$ control (blue) mice were stained with antibodies to CD4, CD8, TCRβ and CD69 and analyzed by flow cytometry. One representantative experiment of 3 is shown.

McCarl et al. Supplemental Figure 7

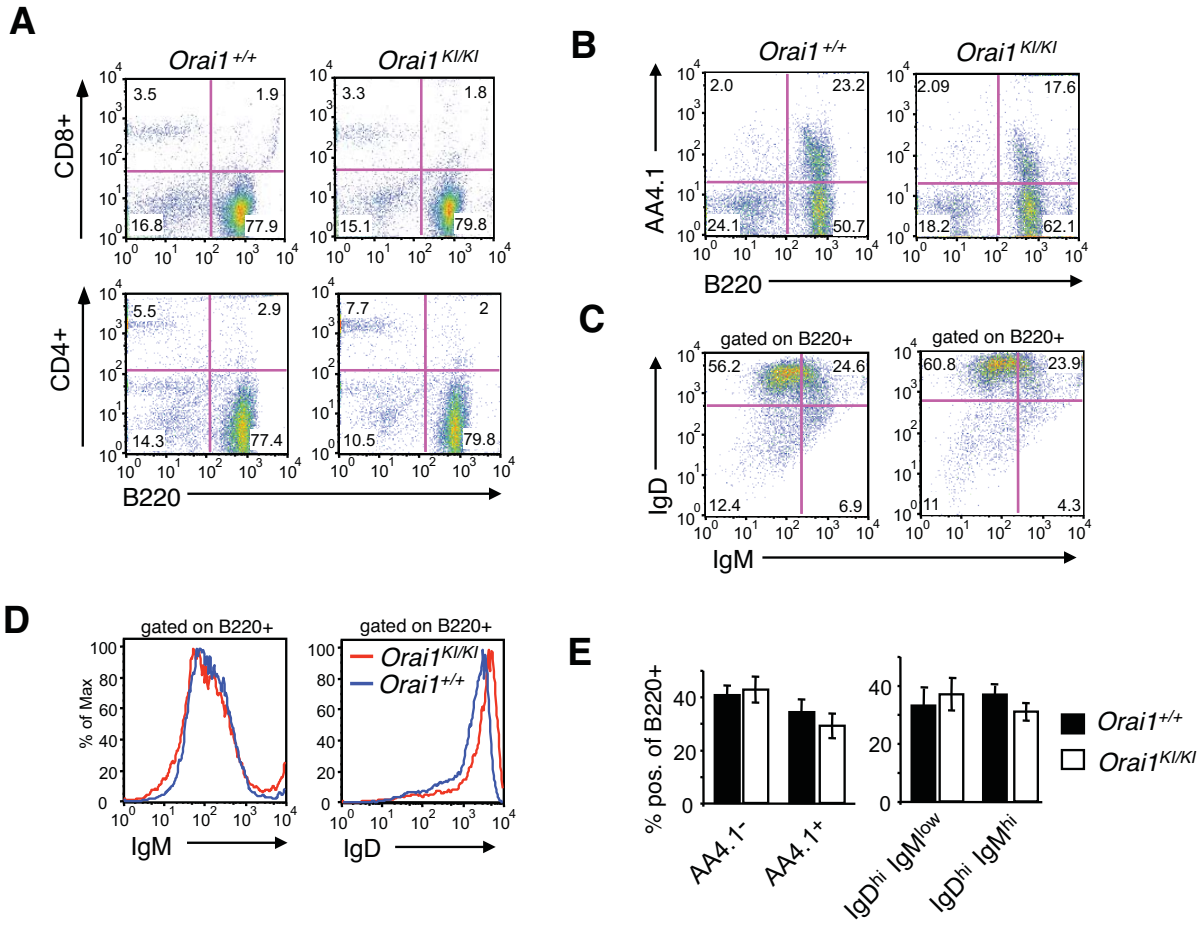

Normal B cell maturation in the spleen of *Orai1*$^{KI/KI}$ mice.

A, Normal T and B cell ratios in spleen of *Orai1*$^{KI/KI}$ mice. Splenocytes of *Orai1*$^{KI/KI}$ and *Orai1*$^{+/+}$ control mice were stained with antibodies to CD4, CD8 and B220. One representative experiment of 7 is shown. For a quantification of lymphocyte populations in spleen and lymph nodes see Figure 1G. **B-E**, Normal B cell maturation in the spleen of *Orai1*$^{KI/KI}$ mice. Splenocytes of *Orai1*$^{KI/KI}$ and *Orai1*$^{+/+}$ control FLC mice were stained with antibodies to AA4.1, B220, IgD and IgM and analyzed by flow cytometry. **B**, Comparable numbers of immature (B220^{+} AA4.1^{+}) and mature (B220^{+} AA4.1^{-}) B cells in *Orai1*$^{KI/KI}$ and *Orai1*$^{+/+}$ control mice. **C-D**, Comparable numbers of immature (B220^{+} IgD^{hi} IgM^{hi}) and mature (B220^{+} IgD^{hi} IgM^{low}) B cells in *Orai1*$^{KI/KI}$ and *Orai1*$^{+/+}$ mice. **E**, Averages of AA4.1, IgD and IgM expression on B220^{+} B cells from *Orai1*$^{KI/KI}$ (n=7) and control (n=7) mice derived from experiments similar to those shown in (B-D). Error bars, SEM.